



# Adsorption kinetics of fluoride on low cost materials

X. Fan\*, D.J. Parker, M.D. Smith

*School of Physics and Astronomy, The University of Birmingham, Birmingham B15 2TT, UK*

Received 9 December 2002; received in revised form 30 June 2003; accepted 1 August 2003

## Abstract

Adsorption is one important technique in fluoride removal from aqueous solutions. The viability of adsorption techniques is greatly dependent on the development of adsorptive materials. A large number of materials have been tested at a fluoride concentration greater than 2 mg/l, and the lowest limit for fluoride reduction by them is about 2 mg/l. Decreasing the fluoride concentration to less than 2 mg/l, most of the tested materials displayed a very low capacity of fluoride removal.

This paper has concentrated on investigating the adsorption kinetics and adsorption capacity of low cost materials at a low initial fluoride concentration. The experiments were carried out at a natural pH, and radioisotope  $^{18}\text{F}$  rather than  $^{19}\text{F}$  was used since  $^{18}\text{F}$  can be rapidly measured by measuring the radioactivity with a resolution of  $1 \times 10^{-13}$  mg or 0.01  $\mu\text{Ci}$ . The tested materials are hydroxyapatite, fluorspar, calcite, quartz and quartz activated by ferric ions. Their adsorption capacities follow the order:

Hydroxyapatite > Fluorspar > Quartz activated using ferric ions > Calcite > Quartz

The uptake of fluoride on hydroxyapatite is an ion-exchange procedure and follows the pseudo-first- and second-order equations, while the uptake of fluoride on the others is a surface adsorption and follows the pseudo-second-order equation. Calcite has been seen as a good adsorbent in fluoride removal and has been patented. However, our data suggested that its adsorption capacity is only better than quartz.

The external mass transfer is a very slow and rate-determining step during fluoride removal from the aqueous solution. Under static conditions, there was no relative movement between adsorbents and solutions, the fluoride uptake was at a very slow rate and the adsorbent properties did not significantly affect the fluoride uptake. Under shaken conditions, the adsorption of fluoride was controlled by the adsorbent structure and chemical properties.

© 2003 Elsevier Ltd. All rights reserved.

**Keywords:** Fluoride; Adsorption kinetics; Hydroxyapatite; Fluorspar; Calcite; Quartz

## 1. Introduction

Fluoride is an essential constituent for both humans and animals depending on the total amount ingested or its concentration in drinking water. The presence of fluorine in drinking water, within permissible limits of 0.5–1.0 mg/l, is beneficial for the production and maintenance of healthy bones and teeth, while excessive intake of fluoride causes dental or skeletal fluorosis

which is a chronic disease manifested by mottling of teeth in mild cases, softening of bones and neurological damage in severe cases [1–4]. Many countries have regions where the water contains more than 1.5 mg/l of fluoride due to its natural presence in the earth's crust, or discharge by agricultural and industrial activities, such as steel, aluminium, glass, electroplating [5–7]. For example, in some regions of North Africa the fluoride concentration of ground water reaches 20 mg/l. In Southern California Lakeland the fluoride concentration in ground water is about 5 mg/l.

Current methods used to remove fluoride from water can be divided into two categories: precipitation and

\*Corresponding author. Tel.: +44-121-4144705; fax: +44-121-4144719.

E-mail address: x.fan@bham.ac.uk (X. Fan).

adsorption. Precipitation of fluoride with calcium and aluminium salts [8,4] has been used to remove fluoride from industrial wastewater. Typically, lime is used as a calcium source, and firstly reduces the fluoride concentration down to 10–20 mg/l. The  $\text{Ca}^{2+}$  ions released from calcium salts interact with fluoride and form  $\text{CaF}_2$  precipitate. Then, aluminium salts are used to reduce the fluoride concentration further to about 2 mg/l [9]. The aluminium salts interact with fluoride in water and form  $\text{AlF}_n^{3-n}$  and  $\text{Al}(\text{OH})_{3-m}\text{F}_m$ , etc. The final concentration of fluoride in the water treated using this method greatly depends on the solubility of precipitated fluorite, as well as calcium and aluminium salts. The solubility of  $\text{CaF}_2$  is theoretically 8 mg/l fluoride at stoichiometric concentrations of calcium; therefore, even when a large dosage of calcium is used, the concentration of fluoride in water is still greater than 2 mg/l [1], and the pH of treated water is at a relatively high value, resulting in a supplementary difficulty of eliminating excess chemicals [10].

Adsorption is another technique, in which fluoride is adsorbed onto a membrane, or a fixed bed packed with resin or other mineral particles. Many techniques have been reported, such as reverse osmosis, electrodialysis, Donnan dialysis, ion exchange, limestone reactor and activated alumina column [11,5]. The efficiency of this technique mainly depends on adsorbents. Among them, ion exchange, electrodialysis and membrane processes are effective and can remove the fluoride to a suitable level, but they are expensive and require frequent regeneration of resin beads or membrane and cleaning of the scaling and fouling [3,5,7,12].

Recent attention of scientists has been devoted to the study of low cost, but effective materials. A large number of materials have been tested, such as activated alumina [13], amorphous alumina [14], activated carbon [3], calcite [15], clay [16], zeolite, charcoal [17], bleaching earth [16], red mud [18]. However, with fluoride concentration decreasing, a lot of adsorbents lose the fluoride removal capacity [19], the lowest limit for fluorine reduction by most of the adsorbents is greater than 2 mg/l [1]; therefore, they are not suitable for drinking water, especially as some of them can only work at an extreme pH value, such as activated carbon which is only effective for fluoride removal at pH less than 3.0 [20].

This paper concentrates on investigating the fluoride adsorption behaviour of materials which are low cost and can effectively remove fluoride from aqueous solutions at a relatively low level. The work was done as part of a programme of developing radioactively labelled particles as tracers for flow studies, but has much wider interest for fluoride removal since the viability of fluoride removal techniques is dependent on the development of adsorptive materials.

## 2. Materials and methods

To compare the adsorption capability of different materials at a low fluoride concentration, the isotope  $^{18}\text{F}^-$  was used in this study instead of  $^{19}\text{F}^-$ . We assume that the behaviour of  $^{18}\text{F}$  is the same as that of  $^{19}\text{F}$  during their adsorption experiments. When  $^{18}\text{F}$  is used, the experiment can be carried out at a very low fluoride concentration, and the adsorption of fluoride on solid particles can be measured immediately and accurately by measuring the radioactivity of  $^{18}\text{F}$  using a radioisotope calibrator CRC-15R (Capintec Inc., NJ), which can detect  $^{18}\text{F}$  at a low amount with a resolution of  $1 \times 10^{-13}$  mg or 0.01  $\mu\text{Ci}$ . The amount of  $^{18}\text{F}$  adsorbed on particles and  $^{18}\text{F}$  concentration ( $C$ ) in aqueous solution can be calculated as

$$N = \frac{A}{\lambda}, \quad (1)$$

$$\lambda = \frac{\ln 2}{t_{1/2}}, \quad (2)$$

$$t_{1/2} = 109.7 \text{ min} = 6582 \text{ s}. \quad (3)$$

Therefore,

$$N = \frac{A}{0.00010531}, \quad (4)$$

$$C = \frac{N}{6.02 \times 10^{23}} \times \frac{1000}{V}, \quad (5)$$

where  $N$  is the number of  $^{18}\text{F}$  molecules,  $\lambda$  is the transformation constant,  $A$  is the radioactivity of  $^{18}\text{F}$  (Bq),  $C$  is fluoride concentration ( $M$ ) and  $V$  is the volume of aqueous solutions (l).

In each experiment, 100 mg of solid particles were added into a glass vial, which contained 6 ml deionised water and fluoride. The water was distilled and then deionised to avoid the interference of other anions and cations. The solid materials used were calcite, quartz, quartz activated by  $\text{Fe}^{3+}$ , fluor spar and hydroxyapatite. All of them were highly crystallised material. Their specific surface areas (BET) were 0.057  $\text{m}^2/\text{g}$  for calcite, 0.060  $\text{m}^2/\text{g}$  for quartz, 0.048  $\text{m}^2/\text{g}$  for fluor spar and 0.052  $\text{m}^2/\text{g}$  for hydroxyapatite respectively. Calcite was used as a reference material since it has been reported to be effective in fluoride removal and has been patented [15,21,22].

## 3. Results and discussions

Theoretically, the adsorption of fluoride onto solid particles normally takes three essential steps:

- (a) diffusion or transport of fluoride ions to the external surface of the adsorbent from bulk solution across the boundary layer surrounding

the adsorbent particle, called external mass transfer;

- (b) adsorption of fluoride ions onto particle surfaces;
- (c) the adsorbed fluoride ions probably exchange with the structural elements inside adsorbent particles depending on the chemistry of solids, or the adsorbed fluoride ions are transferred to the internal surfaces for porous materials (intraparticle diffusion).

The slower steps determine the overall uptake rate and are called “rate-determining step”. To investigate the effect of each step separately, the experiments were carried out at static and shaken conditions. Under static condition, the mixture was left for a certain time interval, and then a small amount of the aqueous solution was removed to measure the radioactivity. After measurement, the aqueous solution was carefully put back into the vial along the vial wall to avoid disturbing the bulk solution. Under the shaken conditions, the mixture in the vial was shaken for a certain time using a mechanical shaker. The shaken time intervals were designed as 10 s, 20 s, 30 s, 1 min, 2 min, and so on, to investigate the adsorption kinetics of fluoride. After each shaken interval, 5.5 ml of the aqueous solution was immediately taken out using a pipette, and the solid particles were left in the vial. The 5.5 ml aqueous solution was used to measure the fluoride concentration by measuring the radioactivity. After the measurement, the aqueous solution was then put back into the vial and was shaken for another time interval.

Figs. 1–4 present the adsorption of fluoride onto hydroxyapatite, fluorspar, calcite and quartz under static and shaken conditions. Figs. 5–8 present the adsorption kinetics of fluoride onto the solids at shaken conditions. Comparing the experimental results obtained from the two conditions, it can be seen that fluoride rapidly adsorbed onto quartz, calcite and fluorspar, and reached equilibrium within 2 min at

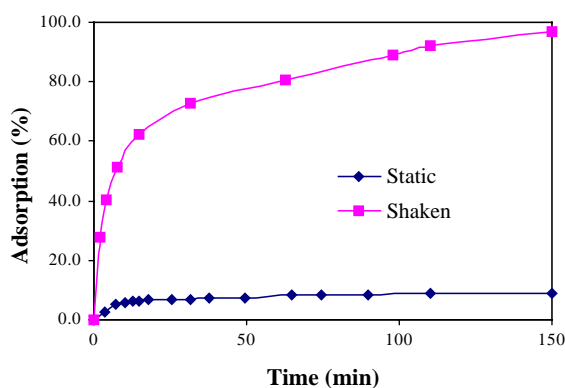


Fig. 1. Adsorption kinetic curves of fluoride on hydroxyapatite with a size range from 212 to 250  $\mu\text{m}$  at pH 6.0 and an initial concentration of  $3 \times 10^{-5}$  mg/l.

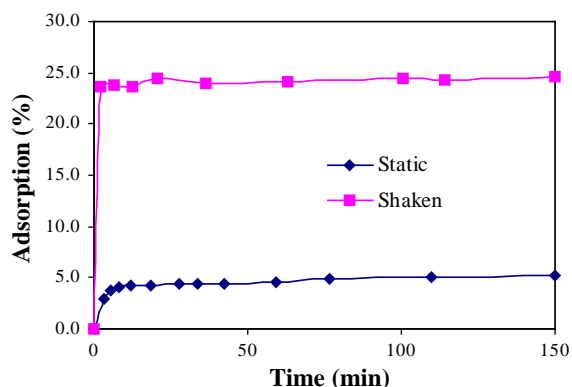


Fig. 2. Adsorption kinetic curves of fluoride on fluorspar with a size range from 212 to 250  $\mu\text{m}$  at pH 6.0 and an initial concentration of  $3 \times 10^{-5}$  mg/l.

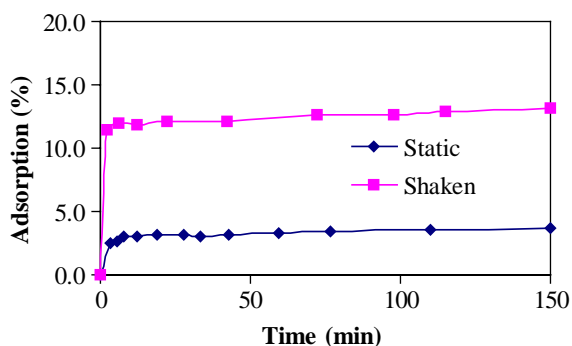


Fig. 3. Adsorption kinetic curves of fluoride on calcite with a size range from 212 to 250  $\mu\text{m}$  at pH 6.0 and an initial concentration of  $3 \times 10^{-5}$  mg/l.

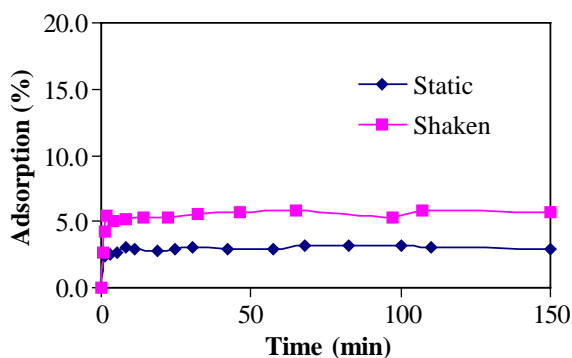


Fig. 4. Adsorption kinetic curves of fluoride on quartz with a size range from 212 to 250  $\mu\text{m}$  at pH 6.0 and an initial concentration of  $3 \times 10^{-5}$  mg/l.

shaken conditions. The adsorption of fluoride on fluorspar, calcite and quartz were  $1.41 \times 10^{13}$  (24% in total),  $3.62 \times 10^{12}$  (12% in total) and  $1.57 \times 10^{12}$  (6% in total) fluoride molecules per gram solid particles with a size range from 215 to 250  $\mu\text{m}$  at an initial fluoride

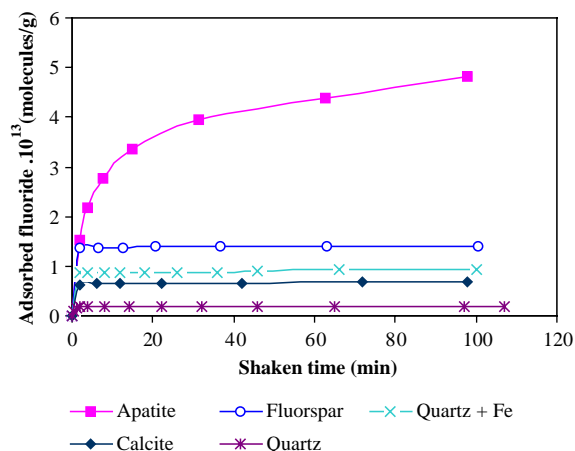


Fig. 5. Adsorbed fluoride molecules on selected materials at pH 6.0 and an initial concentration of  $3 \times 10^{-5}$  mg/l.

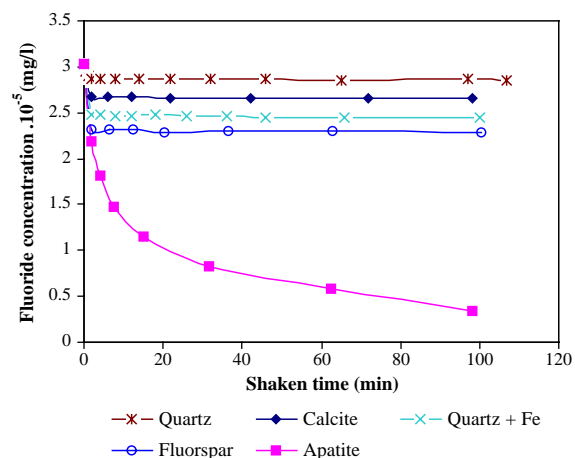


Fig. 6. Variations in fluoride concentrations with time.

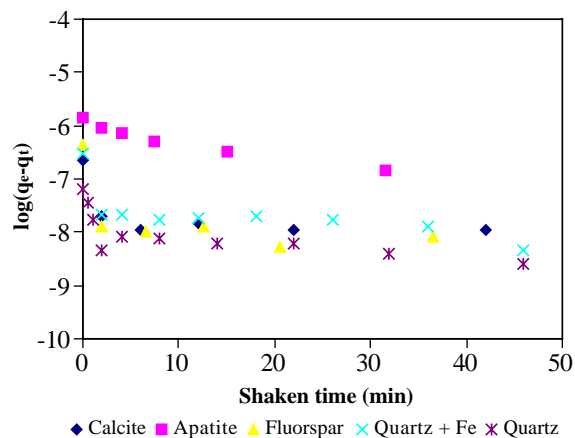


Fig. 7. Pseudo-first-order plot of fluoride adsorption kinetics on the selected materials at pH 6 and an initial concentration of  $3 \times 10^{-5}$  mg/l.

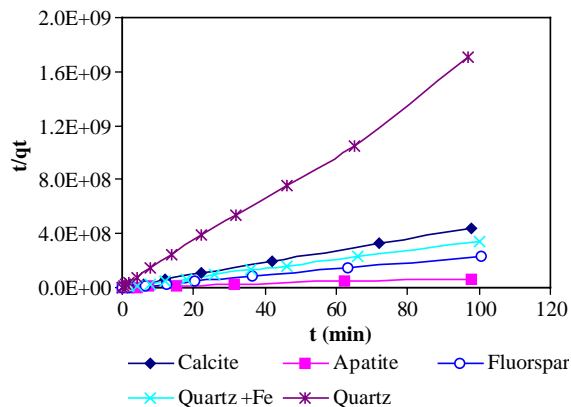


Fig. 8. Pseudo-second-order plot of fluoride adsorption kinetics on the selected materials at pH 6 and an initial concentration of  $3 \times 10^{-5}$  mg/l.

concentration of  $3 \times 10^{-5}$  mg/l respectively. At static conditions, the adsorption of fluoride onto solids was a very slow procedure, and there was no significant difference between hydroxyapatite and the other selected adsorbents. Within the first 10 min, only about 3–6% of fluoride was adsorbed onto all of the four materials, then the adsorption very slowly built up and increased about 2% in 100 min as shown in Figs. 1–4. The adsorption of fluoride onto quartz, calcite and fluorspar took two steps. Fluoride firstly transferred to solid surfaces from bulk solutions and then adsorbed at the active sites. The first step, called external mass transfer of fluoride in the solutions, was very slow and is a rate-determining step. When the mixture was shaken using a mechanical shaker, the solid particle rapidly moved around in the solutions, the concentration of fluoride near solid particle surface could be very close to the bulk concentration. The external mass transfer of fluoride was speeded up, and the equilibrium was reached within 2 min. Shaking or stirring increased the diffusion in the boundary layer and consequently the adsorption rate.

The kinetic analysis of the adsorption data is based on reaction kinetics of pseudo-first-order and pseudo-second-order mechanisms.

Pseudo-first-order adsorption:

$$\frac{dq_t}{dt} = k_1(q_e - q_t). \quad (6)$$

The integrated pseudo-first-order rate equation is written as

$$\log(q_e - q_t) = \log q_e - k_1 t. \quad (7)$$

Pseudo-second-order adsorption:

$$\frac{dq_t}{dt} = k_2(q_e - q_t)^2, \quad (8)$$

$$\frac{d(q_e - q_t)}{(q_e - q_t)^2} = -k_2 dt. \quad (9)$$

Table 1  
Pseudo-first-order rate constants

Material	$K_1$ ( $\text{min}^{-1}$ )	Rate equation	$R^2$
Hydroxyapatite	0.0282	$\log(q_e - q_t) = -0.0282t - 5.9946$	0.9857
Fluorspar	0.0181	$\log(q_e - q_t) = -0.0181t - 7.4775$	0.3579
Calcite	0.0175	$\log(q_e - q_t) = -0.0175t - 7.4271$	0.297
Quartz	0.0202	$\log(q_e - q_t) = -0.0204t - 7.7658$	0.5250
Activated quartz	0.0207	$\log(q_e - q_t) = -0.0207t - 7.3245$	0.4915

Table 2  
Pseudo-second-order rate constants

Material	$K_2$ ( $\text{g min}^{-1} \text{mg}^{-1}$ ) ( $\times 10^6$ )	Rate equation	$R^2$
Hydroxyapatite	0.161	$t/q_t = 695079t + 3 \times 10^6$	0.9977
Fluorspar	8.5	$t/q_t = 2 \times 10^6t + 470598$	1
Activated quartz	3.0	$t/q_t = 3 \times 10^6t + 3 \times 10^6$	0.9996
Calcite	8.33	$t/q_t = 5 \times 10^6t + 3 \times 10^6$	0.9996
Quartz	80.0	$t/q_t = 2 \times 10^7t + 5 \times 10^6$	0.9949

Integrating Eq. (9) at boundary conditions ( $t = 0$  to  $t = t$  and  $q_t = 0$  to  $q_t = q_t$ ) gives

$$\frac{1}{q_e - q_t} = \frac{1}{q_e} + k_2 t, \quad (10)$$

$$\frac{t}{q_t} = \frac{1}{k_2} \frac{1}{q_e^2} + \frac{t}{q_e}, \quad (11)$$

where  $q_e$  and  $q_t$  are the amount of adsorbed fluoride at equilibrium and any time  $t$  ( $\text{mg/g}$  solid material),  $k_1$  ( $\text{min}^{-1}$ ) and  $k_2$  ( $\text{g mg}^{-1} \text{min}^{-1}$ ) are the equilibrium rate constant of first- and second-order sorption respectively, and  $t$  is the shaken time ( $\text{min}$ ).

$k_1$  can be calculated according to the linear plot of  $\log(q_e - q_t)$  versus  $t$ . A larger adsorption rate constant  $k_1$  usually represents a quicker adsorption rate. However, as shown in Fig. 7 and Table 1, only the adsorption data from hydroxyapatite followed the pseudo-first-order equation. The adsorption of fluoride onto calcite, quartz and fluorspar did not follow the pseudo-first-order equation. The correlation coefficients were between 0.30 and 0.53.

$k_2$  can be determined by plotting  $t/q_t$  against  $t$  based on Eq. (11). The larger the  $k_2$  value, the slower the adsorption rate.

All of the kinetic data from the tested materials can be described very well by the pseudo-second-order rate equation as shown in Fig. 8 and Table 2. The correlation coefficients were between 0.998 and 1. At the same initial fluoride concentration ( $3 \times 10^{-5} \text{ mg/l}$ ), the values of the pseudo-second-order rate constants follow the order: hydroxyapatite < quartz activated by ferric ions < calcite < fluorspar < quartz.

The adsorption capacity analysis is based on Langmuir (Eq. (12)) and Freundlich (Eq. (13)) isotherms, and

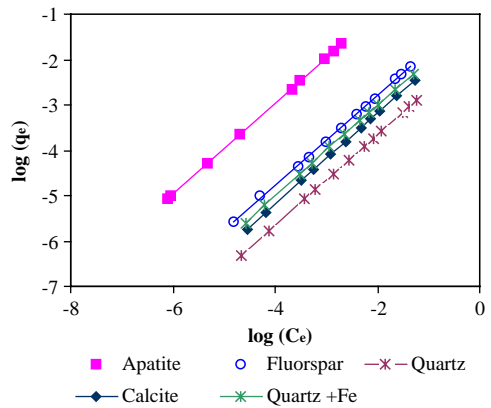


Fig. 9. Freundlich adsorption isotherms of fluoride adsorption.

the results are presented in Figs. 9–11. The experiments for the capacity calculations were carried out at about 10 different initial concentrations in a range from  $2.5 \times 10^{-5}$  to  $6.34 \times 10^{-2} \text{ mg/l}$ . The adsorption times designed for reaching the equilibrium were 180 min for hydroxyapatite and 60 min for quartz, calcite and fluorspar based on the results presented in Fig. 5. The corresponding Langmuir and Freundlich parameters along with correlation coefficients are given in Table 3. The results indicate that the fluoride adsorption data fitted Freundlich isotherm well, and the related correlation coefficients were between 0.999 and 1. But the data did not fit Langmuir isotherm in an initial concentration range from  $2.5 \times 10^{-5}$  to  $6.34 \times 10^{-2} \text{ mg/l}$  since the related correlation coefficients were very low. The adsorption capacities follow the order: hydroxyapatite > fluorspar > quartz activated by ferric ions > calcite > quartz.

Langmuir isotherm:

$$\frac{C_e}{q_e} = \frac{C_e}{Q^0} + \frac{1}{Q^0 b} \quad (12)$$

Freundlich isotherm:

$$\log(q_e) = \log(K_F) + \frac{1}{n} \log(C_e), \quad (13)$$

where  $q_e$  is the adsorbed fluoride at equilibrium (mg/g),  $C_e$  is the fluoride concentration at equilibrium.  $Q^0$  and

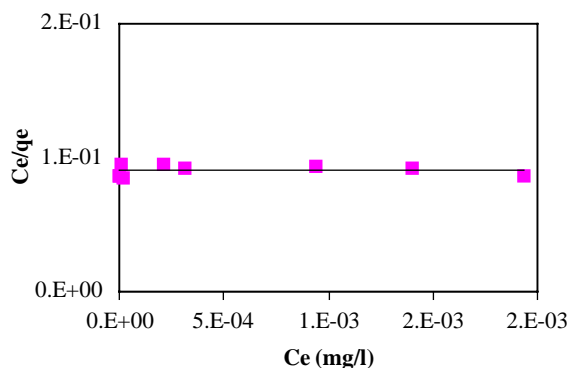


Fig. 10. Langmuir isotherm of fluoride adsorption on hydroxyapatite.

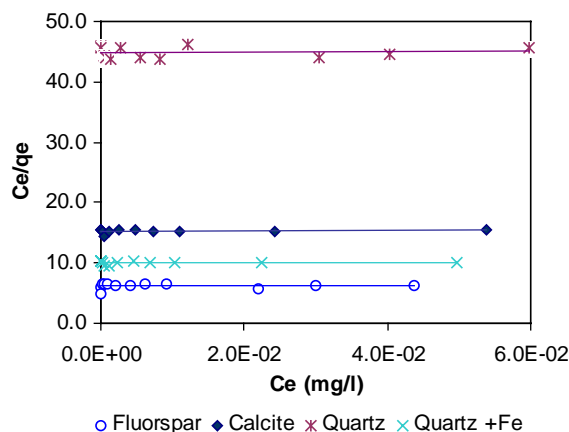


Fig. 11. Langmuir isotherms of fluoride adsorption on fluorspar, calcite and quartz.

$K_F$  are the measurement of the sorption capacity (mg/g) based on Langmuir and Freundlich isotherms respectively,  $b$  is a constant related to the affinity of the binding sites, and  $1/n$  is the adsorption intensity.

Among all the tested materials, hydroxyapatite presented a unique adsorption pattern and the highest fluoride adsorption capacity (Figs. 5,9–11). For example, at an initial fluoride concentration of 0.064 mg/l, the adsorption limits were 0.022 mg/g on hydroxyapatite, 0.0071 mg/g on fluorspar, 0.005 mg/g on activated quartz, 0.0035 mg/g on calcite and 0.0013 mg/g on quartz. The fluoride adsorption equilibrium reached in about 2 min on quartz, calcite and fluorspar, but took much longer time (150 min) on hydroxyapatite.

The hydroxyapatite is a highly crystallised material. Its specific surface area was 0.052 m<sup>2</sup>/g and very close to that of calcite, quartz and fluorspar. The gradual uptake of the fluoride in hydroxyapatite could be due to ion exchange rather than intraparticle diffusion. The fluoride exchanged with some elements inside hydroxyapatite, giving a highest adsorption capacity. Hydroxyapatite Ca<sub>10</sub>(PO<sub>4</sub>)<sub>6</sub>(OH)<sub>2</sub> is the most abundant of phosphatic minerals, and is usually used as a raw material in industrial chemistry. In recent extensive studies, hydroxyapatite was used as bone and tooth implants since its chemical composition and crystallographic structure is similar to those of human hard tissues [23–25]. Hydroxyapatite has the hexagonal structure of fluorapatite but with the OH group displaced from the mirror planes at  $z = \frac{1}{4}$  and  $\frac{3}{4}$ . The disorder of OH<sup>−</sup> ions in  $c$ -axis column gives hydroxyapatite a structural complexity and great scope for substitution for Ca, PO<sub>4</sub> and OH groups [26–28]. The calcium ion can be substituted by metallic ions, such as Pb, Mg, Na, etc. The PO<sub>4</sub> and OH groups can be substituted by some particular anions. Recent studies indicated that hydroxyapatite is an electrically conductive material. The OH group is considered as the charge carrier and can move in an electrical field, even it is a structural element of hydroxyapatite, and forms an hydrogen bond with the nearest of the [PO<sub>4</sub>]<sup>3−</sup> ions [29,24]. In fluoride solution, the fluoride ions firstly adsorbed onto hydroxyapatite surfaces and the adsorbed fluoride exchanged with OH group at nearest

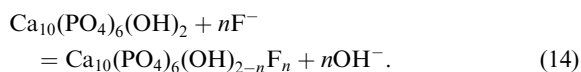
Table 3

Adsorption isotherms of fluoride on the tested materials

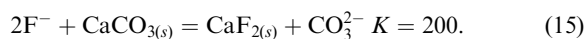
Adsorbent	Langmuir isotherms			Freundlich isotherms		
	$Q^0$	$b$	$R^2$	$K_F$	$n$	$R^2$
Hydroxyapatite	4.54	2.44	0.0015	10.5	1.006	0.999
Fluorspar	1.79	0.091	0.0003	0.15	1.012	0.999
Activated quartz	1.16	0.086	0.0027	0.10	0.999	1
Calcite	0.39	0.023	0.0142	0.066	1.000	1
Quartz	0.19	0.12	0.013	0.023	0.998	1



surface of apatite particles, and then exchanged with the mobile OH group inside hydroxyapatite particles as shown in Eq. (14), resulting in much higher uptake of fluoride on hydroxyapatite.



The uptake of fluoride on quartz, calcite and fluor spar was a surface adsorption process. The amount of adsorbed fluoride rapidly reached a maximum value and equilibrium as shown in Figs. 2–5. The data (Figs. 1–6) did not show that the adsorbed fluoride further exchanged with the structural elements inside of calcite, quartz and fluor spar. Granular calcite has been seen as a good adsorbent to remove fluoride from wastewater. Previous studies showed that, after treating using a fixed bed packed with calcite or one called calcite reactor, the fluoride level in water could be reduced to 4 mg/l [30–32,19,21]. The calcite was considered to work in two ways. Firstly, calcite was considered to be a calcium ion source. Calcite gradually released calcium ions into the water at a certain pH range. The dissolved calcium ions interacted with fluoride in wastewater and formed  $\text{CaF}_2$  precipitate [21,33]. Secondly, the removal of fluoride from the aqueous solution was seen as a pseudomorphic replacement involving epitaxial growth of the (110) plane of fluorite in the (1011) plane of calcite [15]. The fluoride replaced  $\text{CO}_3^{2-}$  from calcite as shown in Eq. (15) and left the  $\text{Ca}^{2+}$  positions nearly unchanged [34].



The volume of  $\text{CaF}_2$  was smaller than that of  $\text{CaCO}_3$ ; the replacement reaction left more porosity; the  $\text{F}^-$  ion could diffuse into the particle and  $\text{CO}_3^{2-}$  could diffuse out of the calcite particles, therefore fluoride could exchange with  $\text{CO}_3^{2-}$  inside calcite [35]. However, our experimental data suggested that among the selected materials, calcite is a fluoride adsorbent which has a poor capacity in fluoride removal at a low fluoride concentration range from  $2.5 \times 10^{-5}$  to  $6.34 \times 10^{-2}$  mg/l, it is only better than quartz. The uptake of fluoride in calcite is a surface adsorption, and rapidly reached equilibrium in 2 min. The fluoride did not appear to further exchange with  $\text{CO}_3^{2-}$  inside calcite particles in the experiment conditions presented in this paper.

Fluor spar ( $\text{CaF}_2$ ) presented the second highest capacity in fluoride removal among the four materials, and adsorbed 25% of fluoride at an initial fluoride concentration of  $3 \times 10^{-5}$  mg/l. It was twice that of calcite. In fluor spar, the Ca and F ions were considered in a sequence of  $\text{F}^-$ – $\text{Ca}^{2+}$ – $\text{F}^-$  triple layers stacking in the [111] direction at a spacing of  $a_0/\sqrt{3} \approx 3.154 \text{ \AA}$  [36]. During crashing, the bonds between calcium and fluorine are broken along its cleavage which is parallel to the [111] plane between adjacent fluorine layers.

Therefore, half of the calcium ions are exposed to the ambient and are active and in an unsaturated state. After calculation of an absolute displacement of  $\Delta r$  which leads to a strong pull of the upper fluorine layer, Dabringhaus [36] suggested it also seemed possible that the strongly distorted fluorine ion of the crystal is exchangeable, can be replaced by other anions. Therefore, the uptake of fluoride on fluor spar could be due to the adsorption of fluoride onto the exposed calcite sites and the strongly distorted fluorine positions of the crystal.

Quartz displayed the poorest  $\text{F}^-$  adsorption capacity. At an initial fluoride concentration of  $3 \times 10^{-5}$  mg/l, the adsorption of fluoride was only  $1.8 \times 10^{12}$  F molecules per gram quartz at equilibrium. However, the activation of quartz using  $\text{Fe}^{3+}$  resulted in a significant increase in fluoride adsorption capacity (Figs. 5, 9 and 11). When the quartz was activated in a  $\text{Fe}_2(\text{SO}_4)_3$  solution of  $5 \times 10^{-3}$  M at pH 6, the adsorption of fluoride onto activated quartz increased from  $1.8 \times 10^{12}$  to  $8.8 \times 10^{12}$  F molecules per gram quartz. In quartz [ $\text{SiO}_2$ ], Si and O are structural elements, the Si–O bond has about 50% covalent character [37]. The siloxane groups,  $-\text{SiOSi}-$ , interact with water forming  $-\text{SiOH}$  [38,39]. The adsorption of fluoride on quartz could be due to a replacement of  $\text{F}^-$  for OH groups on quartz surfaces as shown in Eqs. (16)–(18).



The dramatic increase of fluoride adsorption capacity on the quartz activated using ferric ions could be due to the adsorption of ferric ions on quartz surfaces. Fig. 12 presents the effect of ferric ions on quartz zeta potentials. As the silanol groups are weakly acidic, quartz showed a negative zeta potential above pH 2.6. The zeta potential decreased with increasing the pH

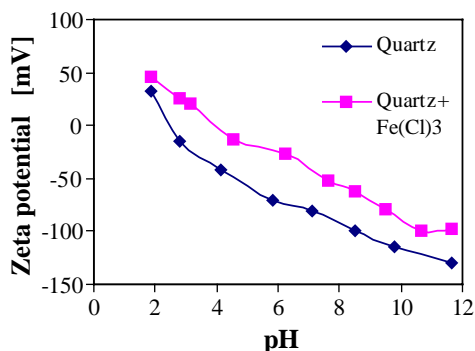


Fig. 12. Effect of  $\text{Fe}^{3+}$  ions on zeta potential of quartz.

value, and reached to about  $-100$  mV at pH 11.5. After activated, the quartz zeta potential increased about 30 mV in the whole range. The increase of quartz zeta potential is due to the adsorption of the ferric ions onto quartz surfaces. The adsorbed ferric ions could act as a bridge to connect fluoride onto quartz surface, and enhance the adsorption of fluoride.

#### 4. Conclusions

Since  $^{18}\text{F}$  is used instead of  $^{19}\text{F}$ , the fluoride adsorption kinetic studies can be carried out at a relatively low concentration in order to investigate low cost materials which can remove fluoride to a lower level.

The external mass transfer is a very slow and rate-determine step during fluoride removal from aqueous solutions. Under static conditions, there was no relative movement between adsorbents and solutions, the fluoride uptake was at a very slow rate and the adsorbent properties did not significantly affect the fluoride uptake. Under shaken conditions, the selected adsorbents moved around in the solutions, the adsorption of fluoride was controlled by the adsorbent structure and chemical properties, and followed the pseudo-second-order equation.

Among the selected materials, the uptake of fluoride was a surface adsorption procedure on calcite, quartz and fluorspar and an ion exchange procedure on hydroxyapatite. Hydroxyapatite has the highest fluoride adsorption capacity. At the initial concentration range from  $2.5 \times 10^{-5}$  to  $6.34 \times 10^{-2}$  mg/l, hydroxyapatite can adsorb over 90% of fluoride at a natural pH (pH = 6). The fluoride was firstly adsorbed onto hydroxyapatite surfaces and then exchanged with OH groups inside the particles. Fluorspar can remove about 25% of fluoride from solution with an initial fluoride concentration range from  $2.5 \times 10^{-5}$  to  $6.34 \times 10^{-2}$  mg/l. Calcite can remove 12% of fluoride and is only better than quartz. The activation of ferric ions on quartz can significantly improve the adsorption capacity of quartz. After the activation, the fluoride removal increased from 5.6% to 20%. Ferric ion was adsorbed on quartz surface and acted as a bridge between quartz and fluoride.

#### References

- [1] Wang Y, Reardon EJ. Activation and regeneration of a soil sorbent for defluoridation of drinking water. *Appl Geochem* 2001;16:531–9.
- [2] Lounici H, Addour L, Belhocine D, Grib H, Nicolas S, Bariou B. Study of a new technique for fluoride removal from water. *Desalination* 1997;114:241–51.
- [3] Srimurali M, Pragathi A, Karthikeyan J. A study on removal of fluorides from drinking water by adsorption onto low-cost materials. *Environ Pollut* 1998;99:285–9.
- [4] Hichour M, Persin F, Sandeaux J, Gavach C. Fluoride removal from waters by Donnan dialysis. *Sep Purif Technol* 2000;18:1–11.
- [5] Amor Z, Malki S, Taky M, Bariou B, Mameri N, Elmidaoui A. Optimization of fluoride removal from brackish water by electrodialysis. *Desalination* 1998;120:263–71.
- [6] Hasany SM, Chaudhary MH. Sorption potential of Haro River quartz for the removal of antimony from acidic aqueous solution. *Appl Radioactive Isot* 1996;47(4): 467–71.
- [7] Cohen D, Conrad HM. 65000 GPD fluoride removal membrane system in Lakeland California USA. *Desalination* 1998;117:19–35.
- [8] Saha S. Treatment of aqueous effluent for fluoride removal. *Water Res* 1993;27:1347–50.
- [9] Yang CL, Dluhy R. Electrochemical generation of aluminium sorbent for fluoride adsorption. *J Hazardous Mater* 2002;2873:1–14.
- [10] Castel C, Schweizer M, Simonnot MO, Sardin M. Selective removal of fluoride ions by a two-way ion-exchange cyclic process. *Chem Eng Sci* 2000;55:3341–52.
- [11] Hichour M, Persin F, Molenat J, Sandeaux J, Gavach C. Fluoride removal from diluted solutions by Donnan dialysis with anion-exchange membranes. *Desalination* 1999;122:53–62.
- [12] Pervov AG, Dudkin EV, Sidorenko OA, Antipov VV, Khakhanov SA, Makarov RI. RO and RF membrane systems for drinking water production and their maintenance techniques. *Desalination* 2000;132:315–21.
- [13] Rubel JF. The removal of excess fluoride from drinking water by the activated alumina method. In: Shupe JL, Peterson HP, Leone NC, editors. *Fluoride effects on vegetation animals and humans*. Salt Lake City: Paragon Press; 1983. p. 345–9.
- [14] Li YH, Wang S, Cao A, Zhao D, Zhang X, Xu C, Luan Z, Ruan D, Liang J, Wu D, Wei B. Adsorption of fluoride from water by amorphous alumina supported on carbon nanotubes. *Chem Phys Lett* 2001;350:412–6.
- [15] Yang M, Hashimoto T, Hoshi N, Myoga H. Fluoride removal in a fixed bed packed with granular calcite. *Water Res* 1999;33(16):3395–402.
- [16] Mahramanlioglu M, Kizilcikli I, Bicer IO. Adsorption of fluoride from aqueous solution by acid treated spent bleaching earth. *J Fluorine Chem* 2002;115:41–7.
- [17] Bhargava DS, Killedar DJ. *Water Res* 1992;26:781.
- [18] Cengeloglu Y, Kir E, Ersoz M. Removal of fluoride from aqueous solution by using red mud. *Sep Purif Technol* 2002;28:81–6.
- [19] Majima T, Takatsuki H. Fluoride removal from smoke-washing wastewater by using  $\text{CaF}_2$  separating method. *Water Purif Liquid Wastes Treatment* 1987;28(7):433–43.
- [20] McKee RH, Jhonston WS. Removal of fluoride from drinking water. *Ind Eng Chem* 1934;26(8):849–50.
- [21] Reardon EJ, Wang Y. Limestone reactor for fluoride removal from wastewaters. *Environ Sci Technol* 2000;34(15):3247–53.



- [22] Hasany SM, Chaudhary MH. Sorption potential of Haro River quartz for the removal of antimony from acidic aqueous solution. *Appl Radioactive Isot* 1996;47(4):467–71.
- [23] Suchanek W, Yoshimura M. Processing and properties of hydroxyapatite-based biomaterials for use as hard tissue replacement implant. *J Mater Res* 1998;13:94–117.
- [24] Laghzizil A, Elherch N, Bouhaouss A, Lorente G, Coradin T, Livage J. Electrical behaviour of hydroxyapatites  $M_{10}(PO_4)_6(OH)_2$  ( $M = Ca, Pb, Ba$ ). *Mater Res Bull* 2001;36:953–62.
- [25] Kim HW, Noh YJ, Koh YH, Kim HE, Kim HM. Effect of  $CaF_2$  on densification and properties of hydroxyapatite-zirconia composites for biomedical applications. *Biomaterials* 2002;23:4113–21.
- [26] McConnell D. Apatite—Its crystal chemistry, mineralogy, utilization, and geologic and biologic occurrences. *Wien, New York: Springer*; 1973. p. 22–32.
- [27] Kay MI, Young RA, Posner AS. *Nature* 1964;204:105.
- [28] Fleet ME, Liu X, Pan Y. Site preference of rare earth elements in hydroxyapatite  $[Ca_{10}(PO_4)_6(OH)_2]$ . *J Solid State Chem* 2000;149:391–8.
- [29] Andres-Verges M, Higes-Rolando FJ, Gonzalez-Dias PF. *J Solid State Chem* 1982;43:237.
- [30] Augustyn W, Dziegielewska A, Kossuth A, Librant Z. Studies of the reaction of crystalline calcium carbonate with aqueous solutions of  $NH_4F$ ,  $KF$  and  $NaF$ . *J Fluorine Chem* 1978;12:281–92.
- [31] Simonsson D. Reduction of fluoride by reaction with limestone particles in a fixed bed. *Ind Eng Chem Process Des Dev* 1979;18(2):288–92.
- [32] Ekdunge P, Simonsson D. Treatment of ammonium fluoride solutions in a semicontinuous fixed bed process. *J Chem Tech Biotechnol* 1984;34A:1–9.
- [33] Kust Roger N, Mishra S, Pfeiffer James B, United States Patents, 5403495.
- [34] Glover ED, Sippel RF. Experimental pseudomorphs: replacement of calcite by fluorite. *Am Mineral* 1962; 47(9-10):1156–65.
- [35] Trautz OR, Zaparta RR. Experiments with calcium carbonate phosphates and the effect of topical application of sodium fluoride. *Arch Oral Biol Spec Suppl* 1961;4:122–33.
- [36] Dabringhaus H. Theoretical study of the adsorption of lithium fluoride molecules at the (1 1 1) surface of  $CaF_2$ . *Surf Sci* 2000;462:123–34.
- [37] Laskowski JS, Ralston J. *Colloid chemistry in mineral processing*. New York: Elsevier; 1992.
- [38] Ralston J, Fornasiero D, Mishchuk N. The hydrophobic force in flotation—a critique. *Colloids Surf A: Physicochem Eng Aspects* 2001;192:39–51.
- [39] Xie X, Morrow NR. Wetting of quartz by oleic/aqueous liquids and adsorption from crude oil. *Colloids Surf A: Physicochem Eng Aspects* 1998;138(1): 97–108.